

Inorganic CuBiS₂ NPs-based Photosensitized ZnO NRs for Solar cell application: Effect of volumetric ratio

Pasupula Ganga Shekar, Ekar SU and Mane RS

¹PG and Research Center, Dept. of Physics, Abasaheb Garware College, Pune 411 004

²Department of Physics, Laxamrao Apte College, Apte Road, Pune 411004, ²Department of Physics, KKM College, Manwat, Parbhani 431505

Email: smragc@rediffmail.com

Manuscript Details

Available online on <http://www.irjse.in>
ISSN: 2322-0015

Editor: Dr. Arvind Chavhan

Cite this article as:

Pasupula Ganga Shekar, Ekar SU and Mane RS
Inorganic CuBiS₂ NPs-based Photosensitized ZnO NRs for Solar cell application: Effect of volumetric ratio, *Int. Res. Journal of Science & Engineering*, January 2018; Special Issue A2: 260-266.

© The Author(s). 2018 Open Access

This article is distributed under the terms of the Creative Commons Attribution 4.0 International License

(<http://creativecommons.org/licenses/by/4.0/>), which permits unrestricted use, distribution, and reproduction in any medium, provided you give appropriate credit to the original author(s) and the source, provide a link to the Creative Commons license, and indicate if changes were made.

ABSTRACT

In the present report; we have discussed inorganic CuBiS₂ NPs-based photosensitized ZnO NRs on ITO substrate. ZnO nanorods (NRs) have been grown by using simple seeding layer and chemical bath deposition (CBD) methods. Inorganic CuBiS₂ NPs with varying volumes of copper, bismuth at the rate of 2.5 mL and keeping the volume of sulphur constant equal to the sum volumes of copper and bismuth have been deposited on seeding layer and CBD deposited ZnO NRs at lower temperatures. The structural elucidation of as prepared CuBiS₂ NP_s-ZnO films have been determined by XRD (X-ray diffraction) and energy dispersive X-ray analysis (EDAX). The films were characterized by UV and Energy band gap analysis and observed that when the Bi-volume was greater than the Cu-volume, then increase in band gap was observed. The CuBiS₂ NP_s-ZnO electrodes have been examined for solar cell application and the maximum conversion efficiency (η) of the film has been determined as 0.278 % for Cu-volume 7.5 mL and Bi-volume 5 mL than the remaining cases of CuBiS₂ and bare ZnO. The electrochemical impedance spectroscopy (EIS) studies of solar cell have been discussed to study the charge transportation. The present work is novel.

Keywords - Seeding layer, CBD, ZnO NRs, Inorganic CuBiS₂ NP_s, Photo-sensitized solar cell.

INTRODUCTION

Presently researchers are attracting towards the development of heterostructured solar cells using wide band gap metal oxides combined with narrow band gap inorganic metal chalcogenide semiconductors. In the visible and infra-red regions of the solar spectrum, many photons are available with the energy lesser than 3 eV. The narrow band gap materials such as CdX, Cu₂X, Bi₂X₃ (X=S or Se) are able to absorb both UV and visible light. But the wide band gap materials such as and Zinc oxide (ZnO) can absorb only UV light. Utilizing both UV and visible lights by combining the narrow band gap inorganic semiconductors with wide band gap ZnO or TiO₂ many researches have been done so far to develop the efficient heterostructure solar cells. Among many metal oxides, like SnO₂, CdO, TiO₂, MgO which have been tested for dye-sensitizing properties, ZnO has received much attention owing to its band gap energy (3.4 eV), which is similar to TiO₂ (3.2 eV) [1]. With wurtzite structure, high photosensitivity, high electron mobility at room temperature, ZnO finds many applications in various fields such as, gas sensor [2], opto-electronics and nanosensor [3], photo detectors [4], piezoelectrics [5], light-emitting diode [6], solar cells [1] and so on. ZnO a II-VI semiconductor with a direct and wide band gap nature exhibits various types of surface morphologies like nano-spikes and nanopillars [7], nano-seeds [8], nano-plates [9], nano-tubes [10], nano-rods [3,10] and so on. The ZnO can be prepared by many types of synthesis techniques that have been developed so far such as, electrodeposition [7], hydrothermal [8], chemical bath deposition (CBD) [2,9], spray pyrolysis [11], sol-gel process [12], SILAR (successive ionic layer adsorption and reaction) [13], and so on. Narrow band gap inorganic NPs sensitised solar cells are being studied due to their certain properties like easy fabrication, possibility to realize more light absorption in the solar spectrum. So far many researchers have reported with the combination of wide band gap semiconductor as photo-anode and narrow band gap inorganic NPs such as ZnO/Bi₂S₃ [14,15], ZnO/Cu₂S [14,16], PbS/ZnO [17], ZnO/GaAs [18], ZnO/CdTe [19], ZnO/CdS [20], and ZnO/CdSe [21], and so on by using various methods. The inorganic narrow band gap NPs like copper based ternary compounds such

as CuSbS₂, CuSbSe₂, CuBiS₂, and CuBiSe₂ have been realized to be possible alternative solar absorbing materials. It was reported that the energy band gaps to be 1.3 eV for CuBiSe₂, 1.4 eV for CuBiS₂, 1.5 eV for CuSbSe₂, and 1.7 eV for CuSbS₂ respectively [22-24]. Of these ternary compounds, CuBiS₂ (Copper bismuth disulphide) finds many applications in thin film lithography, PECs (Photo-electrochemical cells), solar absorber coatings, and so on. To the best of our knowledge very few methods have been developed so far such as CBD [25], spray pyrolysis [26] for the deposition of CuBiS₂. There are many reports available with the combination of wide band gap ZnO and binary metal chalcogenides. But as per our knowledge there are no reports available with the combination of ternary CuBiS₂ NPs with ZnO where an attempt is made in this report.

MATERIALS AND METHODS

2.1: Synthesis of ZnO NRs on bare ITO: The ZnO NRs were grown on ITO by using seeding layer and CBD methods. Initially seeding layer was used to deposit the ZnO on bare ITO and then CBD method was followed. To prepare ZnO solution, Zinc nitrate hexahydrate (Zn(NO₃)₂·6H₂O) was taken in a beaker to which DDW (Double distilled water) and small amount of aqueous ammonia (NH₄OH) were added. By adding NH₄OH drop wise, the solution becomes clear at pH~10.5. Using seeding layer method, the ZnO NRs were grown on ITO by immersing it in ammonia complexed zinc nitrate hexahydrate ([Zn(NH₃)₄]²⁺) precursor kept at room temperature, and in hot DDW (H₂O) maintained at ~88 °C (±2) periodically for few cycles. To grow the ZnO NRs on pre-seeded ZnO substrate by CBD method, Zn precursor solution was prepared as described in the above case. The pre-seeded ZnO substrate was introduced in zinc precursor solution and the beaker was placed in the water bath which was maintained at ~88 °C (±2) for 90 min [13, 15, 27]. After 90 min the substrate with whitish film was removed and rinsed with DDW to remove the loosely bond hydroxide ions and dried in air. CBD second deposition was repeated to get the appropriate thickness of the film.

Table 1: Volumetric ratios of $\text{Cu}(\text{NO}_3)_2 \cdot 3\text{H}_2\text{O}$; $\text{Bi}(\text{NO}_3)_3 \cdot 5\text{H}_2\text{O}$ and $(\text{NH}_2)_2\text{SC}$ reaction process.

Beaker No	Volume of the Solution (mL)			Volumetric ratio	Total Volume (mL)
	Copper Nitrate Tri-Hydrate	Bismuth Nitrate Penta-Hydrate	Thiourea		
1	10	2.5	12.5		
2	7.5	5	12.5	$\text{Cu}_{(7.5)}\text{Bi}_{(5)}\text{S}_{2(12.5)}$	25
3	5	7.5	12.5	$\text{Cu}_{(5)}\text{Bi}_{(7.5)}\text{S}_{2(12.5)}$	25
4	2.5	10	12.5	$\text{Cu}_{(2.5)}\text{Bi}_{(10)}\text{S}_{2(12.5)}$	25

2.2.: Preparation of Cu-Bi-S Stock Solutions: The deposition of CuBiS_2 NPs with volumetric ratio of Cu, Bi, and S by CBD on ZnO deposited ITO (Indium tin oxide) was discussed below. For this $\text{Cu}(\text{NO}_3)_2 \cdot 3\text{H}_2\text{O}$ (Copper nitrate tri hydrate), $\text{Bi}(\text{NO}_3)_3 \cdot 5\text{H}_2\text{O}$ (Bismuth nitrate penta hydrate) and $(\text{NH}_2)_2\text{SC}$ (Thiourea) were used as the sources for Cu, Bi and S and $\text{Cu}(\text{NO}_3)_2 \cdot 3\text{H}_2\text{O}$; $\text{Bi}(\text{NO}_3)_3 \cdot 5\text{H}_2\text{O}$, and $(\text{NH}_2)_2\text{SC}$ stock solutions in the molar ratio of 0.1:0.05:0.1M were prepared at room temperature as discussed below. Initially in a beaker $\text{Cu}(\text{NO}_3)_2 \cdot 3\text{H}_2\text{O}$ solution was prepared by using 48 mL DDW and 2 mL TEA (Tri-Ethano-Amine) was added while the solution was under stirring at 600 rpm stirring at room temperature. To optimize the pH, few sodium hydroxide (NaOH) pellets were added slowly under constant stirring. Further in a separate beaker $\text{Bi}(\text{NO}_3)_3 \cdot 5\text{H}_2\text{O}$ chemical was dissolved using concentrated HNO_3 (Nitric acid) (~1.5 mL) followed by 12 mL DDW and kept the beaker on the magnetic stirrer at 500 rpm stirring at room temperature. After 15-25 min, 2.5 mL TEA was added as a complexing agent followed by the addition of DDW to make 50 mL solution, while the solution was under stirring. The reaction takes place slowly. After 55 min, when the solution was stirring, 1 M basic solution of NaOH was added slowly to prepare alkaline solution and the solution becomes clear at alkaline pH. In another beaker $(\text{NH}_2)_2\text{SC}$ solution was prepared by using $(\text{NH}_2)_2\text{SC}$ chemical and DDW in a beaker. The solution turned to clear in a short interval of time.

2.3: Deposition of CuBiS_2 NPs by CBD on ZnO deposited ITO: $\text{Cu}(\text{NO}_3)_2 \cdot 3\text{H}_2\text{O}$, $\text{Bi}(\text{NO}_3)_3 \cdot 5\text{H}_2\text{O}$ and $(\text{NH}_2)_2\text{SC}$ solutions were taken in 4 separate beakers in the volumetric ratio to prepare 25 mL of Cu-Bi-S mixed solution in each beaker as shown in Table (1). Now, previously deposited ZnO-ITOs were dipped in

these mixed solution beakers. Beakers labelled as No.1 [$\text{Cu}_{(10)}\text{Bi}_{(2.5)}\text{S}_{2(12.5)}$], 2 [$\text{Cu}_{(7.5)}\text{Bi}_{(5)}\text{S}_{2(12.5)}$], 3 [$\text{Cu}_{(5)}\text{Bi}_{(7.5)}\text{S}_{2(12.5)}$], and 4 [$\text{Cu}_{(2.5)}\text{Bi}_{(10)}\text{S}_{2(12.5)}$], (Where, the subscripts in the brackets indicate the volumes of Cu, Bi and S respectively) were kept in the water bath at 62 °C temperature for about 65 min. After the deposition, the films with dark black colour were removed and washed with DDW and dried in air. The as-deposited films were annealed at 200 °C for 60 min and used for the characterization.

RESULTS AND DISCUSSION

3.1: Structural Elucidation:

The structural properties of the CuBiS_2 NPs sensitised ZnO-ITO films were studied from the X-ray diffraction (XRD) patterns recorded by using an X-ray diffractometer with $\text{CuK}\alpha_1$ radiations ($\lambda = 1.5406 \text{ \AA}$) in 2θ range from 20-80 degree. Fig.1 shows the XRD pattern of CuBiS_2 NPs sensitised ZnO-ITO. The XRD peaks of ITO substrate were indicated by asterisk (*). The XRD peaks of ZnO electrodes on ITO were indicated by ZnO revealing the nanostructure well-aligned growth wurtzite (hexagonal) ZnO NRs [JCPDS No: 36-1451]. All the peaks give the hexagonal ZnO NRs structure. Fig.1 (a) characterises the diffraction peaks centred at $2\theta = 24.89^\circ$, 56.30° , 67.61° and at 68.94° be indexed to the (004), (314), (322) and (317) crystal planes, correspond to $\text{Cu}_{(10)}\text{Bi}_{(2.5)}\text{S}_{2(12.5)}$ NPs [JCPDS NO: 43-1473] respectively. Fig. 1(b) characterises the diffraction peaks centred at $2\theta = 24.87^\circ$, 32.78° , 56.45° , and at 67.88° be indexed to the (004), (113), (314) and (322) crystal planes, correspond to $\text{Cu}_{(7.5)}\text{Bi}_{(5)}\text{S}_{2(12.5)}$ NPs [JCPDS NO: 43-1473] respectively. Fig.1(c) characterises the diffraction peaks centred at $2\theta = 25.16^\circ$, 53.09° , 56.38° , 67.85° , and

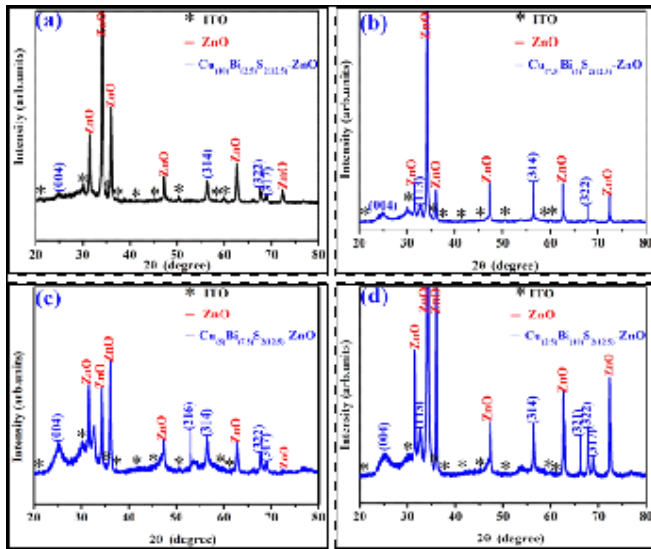


Fig. 1: XRD images of CuBiS₂ NP_s sensitised ZnO electrodes

at 68.98° be indexed to the (004), (216), (314), (322) and (317) crystal planes correspond to Cu₍₅₎Bi_(7.5)S_{2(12.5)} NP_s [JCPDS NO: 43-1473] respectively. Fig.1 (d) characterises the diffraction peaks centred at 2θ=25.28°, 32.54°, 56.27°, 66.25°, 67.81°, and at 68.83° be indexed to the (004), (113), (314), (321), (322), and (317) crystal planes correspond to Cu_(2.5)Bi₍₁₀₎S_{2(12.5)} NP_s respectively [JCPDS NO: 43-1473]. All the peaks of CuBiS₂ NP_s in CuBiS₂ NP_s sensitised ZnO electrodes give the orthorhombic crystal structure.

The presence of elements was identified by using energy dispersive X-ray (EDAX) spectroscopy joined with FE-SEM unit in the CuBiS₂ NP_s sensitised ZnO electrodes heterostructure. Fig. (2) shows the EDAX spectra of the Cu₍₁₀₎Bi_(2.5)S_{2(12.5)}-ZnO, Cu_(7.5)Bi₍₅₎S_{2(12.5)}-ZnO, Cu₍₅₎Bi_(7.5)S_{2(12.5)}-ZnO, and Cu_(2.5)Bi₍₁₀₎S_{2(12.5)}-ZnO films. The spectrum shows solid evidence for the existence of Zn, O, Bi, Cu and S elements in Zn-O and Cu-Bi-S respectively.

3.2: UV analysis and Energy Band gap Study:

Fig. 3 describes the absorption spectra and energy band gaps of ZnO and CuBiS₂ NP_s sensitised ZnO samples studied by using a UV-vis spectrophotometer (WantechWPG-100 Potentiostat /Galvanostatic) in the wavelength range between 350-650 nm for varying volumes of Cu, Bi and keeping the volume of the S constant. The absorption spectra of ZnO and CuBiS₂

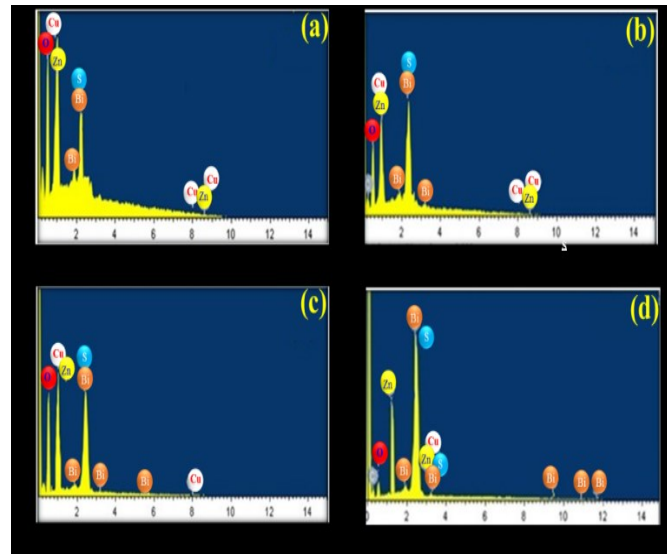


Fig. 2: EDAX images of CuBiS₂ NP_s sensitised ZnO electrodes

NP_s sensitised ZnO electrodes were studied and the absorption data were analysed to estimate the energy band gap by using the Tuac’s relationship. Fig. 3(a) shows the absorbance peaks of ZnO and CuBiS₂ NP_s sensitised ZnO electrodes. As prepared ZnO nano rod film shows good absorbance for 350<λ<400 nm [Fig 3: {a(A)}]. In visible region, CuBiS₂ NP_s sensitised ZnO electrode heterojunction shows good absorbance for 400<λ<475 nm and low absorbance above 450 nm [Fig 3: {a (B-E)}]. Thus CuBiS₂ NP_s sensitised ZnO heterostructure absorbs both visible and UV light indicating the wide range of absorption of light.

The relationship between “α” and “hv” is given by,

$$\alpha = \frac{\alpha_0 (hv - E_g)^n}{hv} \tag{1}$$

Where α = absorption coefficient, E_g = optical band gap, v=frequency of light, h = plank’s constant, hv = photon energy, n = constant.

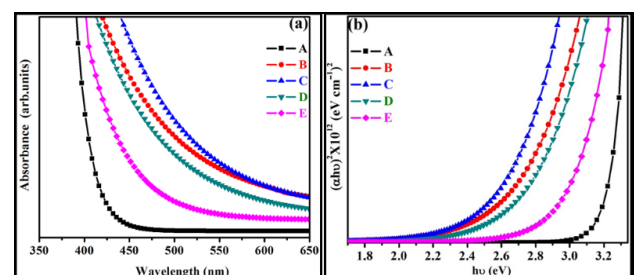


Fig 3: (a) UV and (b) Energy band gap images of ZnO and CuBiS₂ NP_s sensitised ZnO electrodes

[Fig. 3 (b)] depicts the Tauc's plot for ZnO [Fig 3: {b(A)}] and CuBiS₂ NP_s sensitised ZnO electrodes [Fig 3: {b(B-E)}]. The Tauc's plot of $(\alpha h\nu)^2$ versus $h\nu$ is linear and x-intercepts of the plot $(\alpha h\nu)^2$ versus $h\nu$ (photon energy) illustrates the optical band gaps for ZnO and CuBiS₂ NP_s sensitised ZnO. The energy band gap values have been given in Table (2). From Fig. 3 (b) it can be understood that the band gap of Cu_(7.5)Bi₍₅₎S_{2(12.5)}-ITO was observed to be lower than the remaining cases of CuBiS₂ NP_s sensitised ZnO electrodes and ZnO. Thus it can be concluded that when Bi volume was higher than Cu volume and sum volumes of copper and bismuth equal to S volume constantly, the increased energy band gap can be observed.

Table 2: Energy band gap values of ZnO and CuBiS₂-ZnO electrodes.

S.NO.	Compound	Band gap (eV)
A	ZnO-ITO	3.19
B	Cu ₍₁₀₎ Bi _(2.5) S _{2(12.5)} -ITO	2.49
C	Cu _(7.5) Bi ₍₅₎ S _{2(12.5)} -ITO	2.45
D	Cu ₍₅₎ Bi _(7.5) S _{2(12.5)} -ITO	2.56
E	Cu _(2.5) Bi ₍₁₀₎ S _{2(12.5)} -ITO	2.89

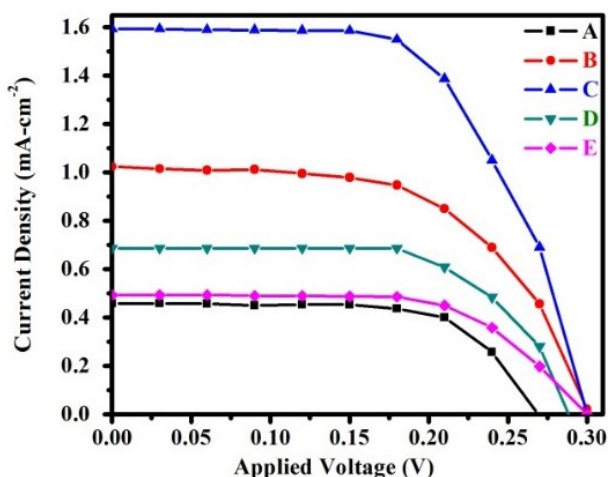


Fig. 4: JV analysis images of ZnO and CuBiS₂ NP_s sensitised ZnO electrodes.

3.3: Photo-Electrochemical Measurement :

The J-V characteristics for the devices under dark and illumination conditions of light were performed using Solar Simulator (with IGOR program and Keithley-2400 power sources meter) [Fig.4]. Under dark, the

non-changing behaviour of curve upto 0.30 V indicates the formation of the good heterojunction of the formed device. Under illumination, the output photovoltaic performance i.e. the short circuit photocurrent density (J_{sc}), open-circuit photo voltage (V_{oc}), fill factor (FF) and power conversion efficiency (η) of the device were calculated. It was observed that the obtained solar cell efficiency of 0.278% [Fig.4 (C)] was observed to be higher than ZnO and the remaining cases of CuBiS₂ sensitized ZnO electrodes [Fig.4.(A, B, D, and E)]. Due to lower band gap, CuBiS₂-ZnO electrodes could absorb more number of photons than bare ZnO which led to the generation of higher number of electron-hole pairs and hence, improved solar cell power efficiency was obtained. Hence, CuBiS₂-ZnO heterostructure electrode showed improved solar cell performance than bare ZnO. Moreover when Cu volume is smaller than Bi volume, more efficiency was observed. Solar cell parameter values for all the electrodes are listed in Table 3.

Table 3: Photovoltaic parameters of photo electrochemical cells composed of CuBiS₂-ZnO electrodes.

Working electrode	V_{oc} (V)	J_{sc} (mA-cm ⁻²)	FF (%)	Efficiency (%)
A	0.27	0.46	0.67	0.083
B	0.30	1.03	0.55	0.171
C	0.30	1.60	0.58	0.278
D	0.29	0.70	0.65	0.131
E	0.30	0.50	0.63	0.095

3.4: Electrochemical Impedance Spectroscopy Measurement:

The most important electronic and ionic phenomena in the solar cell can be investigated by using electrochemical impedance spectroscopy or EIS technique. In general EIS technique is a principal technique to describe the relation between the capacitance and resistances of the photo-anode materials and to study the charge transportation. Fig.5 represents the Nyquist plots for ZnO and CuBiS₂ NP_s-ZnO electrodes. The Nyquist plot is a graph plotted by taking the real part of the impedance on X-axis (Z') and imaginary part on Y-axis (Z''). The Nyquist plots of ZnO [Fig.5(A)] and Cu₍₁₀₎Bi_(2.5)S_{2(12.5)}-ZnO [Fig.5(B)], Cu_(7.5)Bi₍₅₎S_{2(12.5)}-ZnO [Fig.5(C)], Cu₍₅₎Bi_(7.5)S_{2(12.5)}-ZnO

[Fig.5(D)],and $\text{Cu}_{(2.5)}\text{Bi}_{(10)}\text{S}_{2(12.5)}\text{-ZnO}$ [Fig.5 (E)] electrodes consisting of two arcs in the high and low frequency regions corresponding to charge transfer at counter electrode-electrolyte and electrolyte-photoanodes, respectively. The series resistance values of $\text{CuBiS}_2\text{-ZnO}$ electrodes are given in Table 4.

Table 4: Series resistance values of ZnO and $\text{CuBiS}_2\text{-ZnO}$ electrodes.

Working electrode	R_s ($\Omega\text{-cm}$)
A	41
B	50
C	57
D	61
E	52

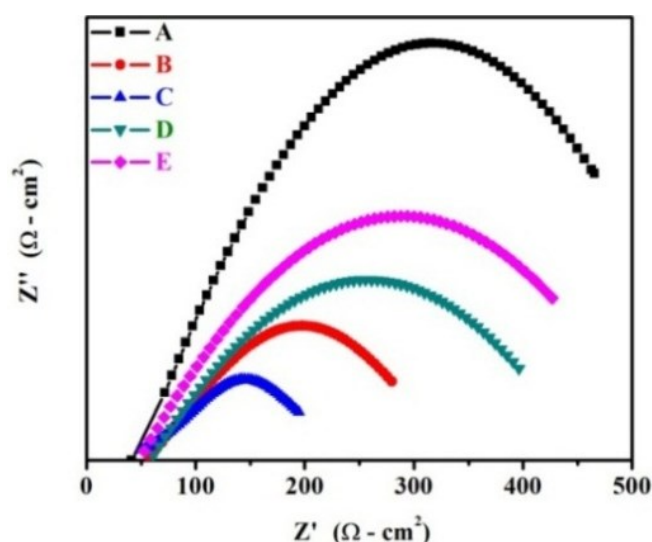


Fig. 5: EIS analysis images of ZnO and CuBiS_2 NPs sensitised ZnO electrodes

CONCLUSION

In summary, we demonstrate the use of simple and inexpensive seeding layer and CBD methods for the ZnO NRs synthesis. Inorganic CuBiS_2 NPs have been sensitised on ZnO electrodes and CuBiS_2 NPs sensitised ZnO electrodes solar cell heterostructure was achieved using CBD method. The present heterostructure of CuBiS_2 NPs-ZnO electrode solar cell has been successfully demonstrated for the solar cell application and observed power conversion efficiency for CuBiS_2 NPs sensitised ZnO electrodes as 0.278 % (for Cu-7.5 mL and Bi-5 mL volumes) which is greater than the remaining cases of Cu-Bi-S-ZnO and ZnO.

REFERENCES

1. R. S. Mane, W. J. Lee, H. M. Pathan, and S. H. Han, Nanocrystalline TiO_2/ZnO Thin Films: Fabrication and Application to Dye-Sensitized Solar Cells, *J. Phys. Chem. B*, 109 (2005) 24254-24259.
2. C.D. Lokhande, P.M. Gondkar, R.S. Mane, V.R. Shinde, S.H. Han, CBD grown ZnO based gas sensors and dye-sensitized solar cells, *Current Applied Physics*, 475 (2009) 304-311.
3. X. D. Wang, C. J. Summers, Z. L. Wang, Large-Scale Hexagonal-Patterned Growth of Aligned ZnO Nanorods for Nano-Optoelectronics and Nanosensor Arrays, *Nano Lett.*, 4 (2004) 423-426.
4. S. Liang, H. Sheng, Y. Liu, Z. Huo, Y. Lu, H. Shen, "ZnO Schottky ultraviolet photodetectors", *J Cryst Growth*, 225 (2001) 110-113.
5. A. Janotti, C.G. Van de Walle, Fundamentals of zinc oxide as a semiconductor, *Reports on Progress in Physics*, 72 (2009) 12650-12658.
6. Jong H. Na, M. Kitamura, M. Arita, and Y. Arakawa, Hybrid p-n junction light-emitting diodes based on sputtered ZnO and organic semiconductors, *Applied physics letters*, 95 (2009) 253303.
7. D. Pradhan, M. Kumar, Y. Ando, K.T. Leung, Fabrication of ZnO nanospikes and nanopillars on ITO glass by template less seed-layer-free electrodeposition and their field-emission properties, *ACS Appl. Mater. Interfaces*, 1 (2009) 789-796.
8. W. B. Wu, G. D. Hu, S. G. Cui, Y. Zhou, H. T. Wu, Epitaxy of Vertical ZnO Nanorod Arrays on Highly (001)-Oriented ZnO Seed Monolayer by a Hydrothermal Route, *Cryst. Growth Des.*, 8 (2008) 4014.
9. B. Cao, W. Cai, From ZnO Nanorods to Nanoplates: Chemical Bath Deposition Growth and Surface-Related Emissions, *The Journal of Physical Chemistry C*, 112 (2008) 680-685.
10. C. S. Rout, S. H. Krishna, S. R. C. Vivekchand, A. Govindaraj, C. N. R. Rao, Hydrogen and ethanol sensors based on ZnO nanorods, nanowires and nanotubes, *Chem. Phys. Lett.*, 418 (2006) 586-590.
11. P. Singh, A. Kaushal, D. Kaur, Mn-doped ZnO nanocrystalline thin films prepared by ultrasonic spray pyrolysis, *Journal of Alloys and Compounds*, 471 (2009) 11-15.
12. W.P. Tai, J.H. Oh, Humidity sensing behaviors of nanocrystalline ZnO thin films by sol-gel process,

- Journal of Materials Science - Materials in Electronics, 13 (2002) 391-394.
13. P. Suresh Kumar, A. Dhayal Raj, D. Mangalaraj, D. Nataraj, Growth and characterization of ZnO nanostructured thin films by a two-step chemical method, *Applied Surface Science*, 255 (2008) 2382-2387.
 14. P. Chen, L. Gu and X. Cao, From single ZnO multipods to heterostructured ZnO/ZnS, ZnO/ZnSe, ZnO/Bi₂S₃ and ZnO/Cu₂S multipods: controlled synthesis and tunable optical and photo electrochemical properties, *Cryst Eng Comm.*, 12 (2010) 3950-3958.
 15. P.R. Nikam, P.K. Baviskar, J.V. Sali, K.V. Gurav, J.H. Kim, B.R. Sankapal, SILAR coated Bi₂S₃ nanoparticles on vertically aligned ZnO nanorods: Synthesis and characterizations, *Ceramics International*, 41 (2015) 10394.
 16. K.Guo,X.Chen,J.Han,Z.Liu,Synthesis of ZnO/Cu₂S core/shell nanorods and their enhanced photoelectric performance, *Journal of sol-gel science and technology*, 72 (2014) 92-99.
 17. J.M. Luther, J. Gao, M.T. Lloyd, O.E. Semonin, M.C. Beard, A.J. Nozik, Stability assessment on a 3% bilayer PbS/ZnO quantum Dot heterojunction solar cell, *Adv. Mater.* 22, (2010) 3704-3707.
 18. P. F. Zhang, X. L. Liu, R. Q. Zhang, H. B. Fan, A. L. Yang, H. Y. Wei, P. Jin, S. Y. Yang, Q. S. Zhu, and Z. G. Wang, Valence band offset of ZnO/GaAs heterojunction measured by x-ray photoelectron spectroscopy, *Applied Physics Letters*, 92 (2008) 012104.
 19. X. Wang, H. Zhu, Y. Xu, H. Wang, Y. Tao, S. Hark, X. Xiao, Q. Li, Aligned ZnO/CdTe core-shell nanocable arrays on indium tin oxide: Synthesis and photoelectrochemical properties, *ACS Nano*, 4 (2010) 3302-3308.
 20. G. Murugadoss, ZnO/CdS nanocomposites: Synthesis, structure and morphology, *Nanotechnology*, 10 (2012) 722.
 21. C. Zhu, X. Pan, C. Ye, L. Wang, Z. Ye, J. Huang, Effect of CdSe quantum dots on the performance of hybrid solar cells based on ZnO nanorod arrays, *Ceram. Int.*, 39 (2013) 2975-2980.
 22. M. Kumar, C. Persson, Cu(Sb,Bi)(S,Se)₂ as indium-free absorber material with high optical efficiency, *Energy Proc.*, 44 (2014) 176-183.
 23. J.T.R. Dufton, A. Walsh, P.M. Panchmatia, L.M. Peter, D. Colombara, M.S. Islam, Structural and electronic properties of CuSbS₂ and CuBiS₂: potential absorber materials for thin-film solar cells, *Physical Chemistry Chemical Physics.*, 14 (2012) 7229-7233.
 24. D.J. Temple, A.B. Kehoe, J.P. Allen, G.W. Watson, D.O. Scanlon, Geometry, electronic structure, and bonding in CuMCh₂ (M = Sb, Bi; Ch = S, Se): alternative solar cell absorber materials?, *J Phys. Chem. C*, 116 (2012) 7334-7340.
 25. P.S. Sonawane, P.A. Wani, L.A. Patil, Tanay Seth, Growth of CuBiS₂ thin films by chemical bath deposition technique from an acidic bath, *Materials Chemistry and Physics*, 84 (2004) 221-227.
 26. S. H Pawar, A. J Pawar, P. N. Bhosale, Spray pyrolytic deposition of CuBiS₂ thin films, *Bull Mater Sci.* 8 (1986) 423-426.
- P. K. Baviskar, P.R. Nikam, S.S. Gargote, A. Ennaoui, B.R.Sankapal, Controlled synthesis of ZnO nanostructures with assorted morphologies via simple solution chemistry, *Journal of Alloys and Compounds*, 551 (2013) 233

© 2018 | Published by IRJSE

Submit your manuscript to a IRJSE journal and benefit from:

- ✓ Convenient online submission
- ✓ Rigorous peer review
- ✓ Immediate publication on acceptance
- ✓ Open access: articles freely available online
- ✓ High visibility within the field

Email your next manuscript to IRJSE

: editorirjse@gmail.com